Title: A novel role for milk fat globule-EGF factor 8 protein (MFGE8) in the mediation of mouse sperm-extracellular vesicle interactions

Authors: Natalie A. Trigg [1,2], Simone J. Stanger [1,2], Wei Zhou [1,2,3,4], David A. Skerrett-Byrne [1,2], Petra Sipilä [5], Matthew D. Dun [6,7], Andrew L. Eamens [1,2], Geoffry N. De Iuliis [1,2], Elizabeth G. Bromfield [1,2], Shaun D. Roman [1,2,8], Brett Nixon [1,2*]

[1] Priority Research Centre for Reproductive Science, School of Environmental and Life Sciences, Discipline of Biological Sciences, The University of Newcastle, University Drive, Callaghan, NSW, Australia

[2] Hunter Medical Research Institute, Pregnancy and Reproduction Program, New Lambton Heights, NSW, Australia

[3] Department of Obstetrics and Gynaecology, The University of Melbourne, Parkville, VIC, Australia

[4] Gynaecology Research Centre, The Royal Women's Hospital, Parkville, VIC, Australia.

[5] Institute of Biomedicine, Research Centre for Integrative Physiology and Pharmacology, and Turku Center for Disease Modeling, University of Turku, Turku, Finland

[6] School of Biomedical Sciences and Pharmacy, Faculty of Health and Medicine, The University of Newcastle, Callaghan, NSW, Australia

[7] Hunter Medical Research Institute, Cancer Research Program, New Lambton Heights, NSW, Australia

[8] Priority Research Centre for Drug Development, The University of Newcastle, University Drive, Callaghan, NSW, Australia

*** Corresponding author:** Brett Nixon (brett.nixon@newcastle.edu.au)

Short title: MFGE8 mediates sperm-extracellular vesicle interaction

Keywords: epididymis, epididymosome, extracellular vesicle, milk fat globule-EGF factor 8 protein (MFGE8), spermatozoa, sperm maturation

SIGNIFICANCE OF THE STUDY

This study focuses on characterizing the receptor-ligand interactions that mediate interactions between mouse spermatozoa and the extracellular vesicles (EV) they encounter within the male reproductive tract (epididymis). To facilitate these studies we describe the optimization of a tractable cell culture system with which to model sperm-EV interactions. In tandem with receptor inhibition strategies, our data demonstrate the importance of the Milk Fat Globule-EGF Factor 8 (MFGE8) protein ligand in mediating the efficient exchange of macromolecular EV cargo with mouse spermatozoa. Overall, these findings shed new light on the mechanistic basis of the EV interactions that underpin sperm maturation with potential applications extending to the diagnosis and treatment of male factor infertility.

ABSTRACT

Spermatozoa transition to functional maturity as they are conveyed through the epididymis, a highly specialized region of the male excurrent duct system. Owing to their transcriptionally and translationally inert state, this transformation into fertilization competent cells is driven by complex mechanisms of intercellular communication with the secretory epithelium that delineates the epididymal tubule. Chief among these mechanisms are the release of extracellular vesicles (EV), which have been implicated in the exchange of varied macromolecular cargo with spermatozoa. Here, we describe the optimization of a tractable cell culture model to study the mechanistic basis of sperm-extracellular vesicle interactions. In tandem with receptor inhibition strategies, our data demonstrate the importance of Milk Fat Globule-EGF Factor 8 (MFGE8) protein in mediating the efficient exchange of macromolecular EV cargo with mouse spermatozoa; with the MFGE8 integrin-binding Arg-Gly-Asp (RGD) tripeptide motif identified as being of particular importance. Specifically, complementary strategies involving MFGE8 RGD domain ablation, competitive RGD-peptide inhibition and antibody-masking of alpha V integrin receptors, all significantly inhibited the uptake and redistribution of EV-delivered proteins into immature mouse spermatozoa. These collective data implicate the MFGE8 ligand and its cognate integrin receptor in the mediation of the EV interactions that underpin sperm maturation.

Words = 198 / 200

INTRODUCTION

Successful fertilization is underpinned by the union of gametes, with each cell having first attained the necessary level of functional maturity [1]. In the case of the spermatozoon, this journey to maturity is initiated within the testes during which time the germline undergoes sequential mitotic and meiotic divisions followed by cytoplasmic and nuclear remodeling to eventually give rise to one of the most highly differentiated cells in the mammalian body [2]. Notwithstanding this morphological transformation, mammalian sperm cells only acquire the acumen to fertilize an ovum during their carriage through the epididymal portion of the male extragonadal duct system [3]. This conversion into fertilization competent cells is accompanied by substantive modification of the sperm proteomic [4] and epigenetic landscapes [5]; processes that occur in the complete absence of nuclear gene transcription and protein translation. Instead, mammalian sperm maturation is driven exclusively by the interplay of sophisticated forms of intercellular communication with the epididymal soma [6]. Chief among these mechanisms is the secretion of extracellular vesicles (EVs), termed epididymosomes, which have been implicated in the exchange of varied forms of macromolecular cargo with spermatozoa [7-10].

Epididymosomes originate within the epithelial cells of the mammalian epididymis as constituents of multivesicular bodies [9], before being shed into the lumen of the duct whereupon they interact with spermatozoa and downstream epithelial cells [11, 12]. The extent to which epididymosomes influence their recipient cells is highlighted by recent compositional analyses, which have revealed these EVs encapsulate a diverse cargo of proteins [13, 14], small non-coding RNAs [7, 11, 15], and lipids [8, 16]. Moreover, the development of tractable *in vitro* co-culture assays has confirmed the transfer of each of these forms of cargo between epididymosomes and spermatozoa [7, 10]. Such assays have also begun to yield important insights into the mechanisms by which epididymosome cargo is exchanged,

revealing the important influences of temperature, pH and ionic concentration [9]. Similarly, a combination of pharmacological intervention and differential labeling strategies has provided evidence that mouse epididymosome-sperm interactions can be resolved into two sequential phases involving rapid tethering followed by a transient membrane fusion and cargo delivery [10]. Despite these advances, we remain uncertain about the full complement of cognate receptor – ligand interactions that mediate the tethering of epididymosomes to the sperm head as well as the signaling pathway(s) that are engaged in response to this interaction. With the intention of bridging this important knowledge gap, here we explore the role of Milk Fat Globule-EGF Factor 8 (MFGE8) protein in the mediation of mouse sperm-EV interactions.

In guiding the target selection for this study, our previous work has demonstrated that antibody masking of epididymosome-resident MFGE8 effectively reduces the ability of these vesicles to bind mouse spermatozoa (Nixon et al., 2019b). This finding builds on evidence that MFGE8 acts as an adhesion molecule responsible for the orchestration of diverse cellular interactions [17]. Such activity has been linked to the presence of an RGD integrin-binding motif, which is capable of engaging αvβ3/5 integrin heterodimers to facilitate cell adhesion and induce integrin-mediated signal transduction [17]. In terms of the male reproductive tract, MFGE8 was originally characterized as a sperm protein with binding affinity for glycoproteins of the egg coat [18]; a function that is conserved in both porcine and mice [19]. It follows that male mice harboring an *Mfge8*-null mutation are sub-fertile, producing spermatozoa that are unable to bind eggs *in vitro* [19]. Notably, mouse sperm first acquire MFGE8 within the Golgi complex of spermatogenic cells, however, the majority of sperm-associated MFGE8 is derived from secretions of the proximal epididymis. Here, we offer mechanistic insight into the mode of MFGE8 transfer to maturing spermatozoa via EVs, and also propose a functional role for the MFGE8 RGD domain in the engagement of αV integrin receptors on spermatozoa.

MATERIALS AND METHODS

Reagents

All reagents were of molecular biology or research grade and unless specified, were obtained from Merck (Burlington, MA, USA) or Thermo Fisher Scientific (Waltham, MA, USA). A summary of all antibodies used this study is provided in Supplementary Table S1.

Ethics Statement

All experimental procedures involving animals were conducted with the approval of the University of Newcastle's Animal Care and Ethics Committee (approval numbers A-2013-322 and A-2018-826), in accordance with relevant national and international guidelines. Swiss mice were housed under a controlled lighting regime (12L: 12D) at 21–22°C and supplied with food and water *ad libitum*. Prior to dissection, animals were euthanized via CO_2 inhalation.

mECap18 cell culture and extracellular vesicle isolation

An immortalized mouse caput epididymal (mECap18) cell line was utilized to harvest EVs under normal *in vitro* incubation conditions [20] and in cells subjected to CRISPR-Cas9 genome editing to generate mutations in the target gene, *Mfge8* (see below). Cells were grown to ~70% confluency, washed three times with sterile phosphate buffered saline (PBS) and incubated in serum free media for 24 h before the collection of conditioned media for EV isolation.

Conditioned media (15 mL) was carefully aspirated and cleared of cellular debris by two sequential centrifugation steps at 500 × *g* and 2000 × *g* for 5 min each at 4°C. The resultant supernatant was concentrated by centrifugation using an Amicon Ultra-15

Centrifugal Filter Unit (30 kDa cut-off; Merck) at 3000 × *g* at 4°C to a volume of ~200 – 400 µL prior to further centrifugation steps at increasing velocity (4000 × *g*, 8000 × *g* and 17,000 × *g* for 15 min at 4°C per centrifugation) to eliminate all traces of cellular debris. The supernatant (~450 µL) was gently overlaid upon a discontinuous iodixanol-based density gradient (comprising 40%, 20%, 10% and 5% suspensions) (OptiPrep; Merck) before being centrifuged at 100,000 × *g* for 18 h at 4°C as previously described [7]. Thereafter, twelve equal fractions (185 µL / fraction) were recovered, diluted in PBS, and subjected to a final ultracentrifugation step at 100,000 × *g* for 3 h at 4°C. The resulting pellets were processed as described below.

mECap18 extracellular vesicle characterization

Initial characterization of fractionated samples focused on confirming the presence of recognized EV markers (FLOT1, CD9, CD63) by immunoblotting according to [7]. The identification of EV markers predominantly within fractions 9 and 10, prompted the pooling of these fractions for all subsequent experiments. EVs were characterized based on mean particle size and heterogeneity via analysis on a Zetasizer Nano ZS (Malvern Instruments, Malvern, UK) [7]. EV morphology, purity and size were also assessed by conventional transmission electron microscopy [7, 21] and by concentration onto aldehyde/sulfate latex beads followed by sequential labeling with anti-FLOT1 and Alexa Fluor 488-conjugated secondary antibodies [7]. Finally, EVs and mECap18 cell lysates were prepared for immunoblotting with a suite of antibodies (CD63, CD9, PSMD7, FLOT1, HSP90B1, APOA1, GAPDH) recommended for EV validation [22].

Proteomic comparison of mECap18 extracellular vesicles and mouse caput epididymosomes

To examine the conservation of the physical characteristics of mECap18 EVs and that of native epididymosomes, the latter were isolated from the caput epididymal tissue of adult male mice as previously described [7, 10]. After isolation, mECap18 EVs and epididymosomes were lysed separately (7 M urea, 2 M thiourea, 4% (w/v) CHAPS for 1 h on ice with regular vortexing) and 40 μg of protein from each vesicle lysate was labeled with 320 pmol of appropriate cyanine-dye reagents (i.e. either Cyanine3 or Cyanine5 esters) for 1 h on ice. Labeling reactions were quenched by addition of excess L-lysine (10 mM, 10 min on ice) after which the differentially labeled samples were combined, resolved by 2D SDS-PAGE and imaged using a ChemiDoc MP imaging system (Bio-Rad, Hercules, CA) [14].

Transfer of extracellular vesicle protein and microRNA cargo to mouse spermatozoa

The interaction of mECap18 EVs with spermatozoa was assessed by biotinylation of their proteomic contents (membrane impermeable: EZ-Link sulfo-NHS-LC-Biotin; membrane permeable: EZ-Link BMCC-Biotin; Thermo Fisher Scientific) as previously described [10]. Labeled EVs were subsequently co-incubated with caput epididymal sperm for 1 or 3 h at 37°C in an atmosphere of 5% CO_2 [10], with visualization of the sperm domains harboring transferred biotinylated cargo being achieved via affinity labeling with Alexa Fluor 488 conjugated streptavidin. Images were captured by confocal microscopy (Olympus FV1000; Olympus, Shinjuku, Tokyo, Japan) and transfer efficiency was assessed by counting the percentage of labeled spermatozoa. Controls to discriminate the specificity of EV mediated protein transfer included naïve populations of unlabeled spermatozoa, sperm labeled directly with biotin, and sperm incubated with unlabeled EVs.

Using an identical co-incubation strategy, we also investigated the exchange of microRNA (miRNA) cargo between EVs and recipient spermatozoa. Following incubation, sperm cells were processed for total RNA extraction as previously described [7]. The

abundance of candidate miRNAs [*miR-191-5p* (assay ID 002299), *miR-375-3p* (assay ID 000564), *miR-467a-5p* (assay ID 001826) and *miR-467e-5p* (assay ID 002568)] was examined by quantitative real-time PCR (RT-qPCR) with TaqMan miRNA assay reagents in accordance with the manufacturer's instructions (Thermo Fisher Scientific). RT-qPCR data was normalized against the U6 small nuclear RNA (snRNA; assay ID 001973) and relative abundance was calculated using the $2^{-\Delta Ct}$ method [23].

Generation of CRISPR-Cas9-mediated *Mfge8* mutant mECap18 cells

All CRISPR-Cas9 reagents were obtained from Thermo Fisher Scientific. Prior to transfection, mECap18 cells were seeded at 150,000 cells/well into 12-well plates without antibiotics. Cells were then transfected with 1,250 ng TrueCut Cas9 Protein v2, 315 ng TrueGuide gRNA (A35510; ID: CRISPR475261_SG), 2.5 µL lipofectamine Cas9 with PLUS solution and 4.0 µL lipofectamine 3,000 as per manufacturer's instructions (Thermo Fisher Scientific). An internal transfection control (mCherry Red) was used to estimate transfection efficiency. Cells were allowed to recover for 24 h at 37°C in 5% CO_2 before being re-seeded into 6-well plates and cultured for 72 h. Transfected cells were harvested and divided for genome editing quantification using a GeneArt Genomic Cleavage Detection Kit (A24372; Thermo Fisher Scientific) with *Mfge8* flanking primers (5′ - CTGGTCTTGGCTCCAAGT - 3′ and 5′ - ATGTGGGCAAACTGATCC - 3′) as per manufacturer's instructions, and the resultant cell population was then replated as single cells in 96-well plates using limited dilution cloning. Resulting colonies were expanded and gDNA Sanger sequencing was performed to detect deletions.

***Mfge8* mutant cDNA transcript validation**

One wild-type and two mutant lines were selected for analysis based on their gDNA sequences and used to characterize the specifics of CRISPR-Cas9-induced deletions. Cells

from these lines were harvested and total cellular RNA (3.0 μg) was reverse transcribed using 500 ng Oligo(dT)15 primer, 5 × buffer, 100 mM dithiothreitol, 40 U RNasin ribonuclease, 0.5 mM dNTPs and 20 Units (U) of Moloney murine leukemia virus reverse transcriptase. Subsequent PCR reactions were performed with the equivalent of 100 ng of RNA, 80 ng of each primer (5′ - GCATGCTACTCTGCGCCTC - 3′ and 5′ – GCTGCTGGGCTGTTAATGCTC - 3′), 0.5 mM dNTPs, 1 U of GoTaq DNA Polymerase (Promega, Madison, WI) and 1.5 mM $MgCl_2$. DNA from PCR products was purified from 1.0% (w/v) agarose gels using a Wizard SV Gel and PCR Clean-Up System (Promega) and cloned into the pGEM-T Easy Vector as per the manufacturer's instructions (Promega). Extracted plasmid DNA was subjected to Sanger sequencing. To ensure equivalent expression of wild-type and mutant *Mfge8* transcripts RT-qPCR analysis was performed using GoTaq qPCR Master Mix (Promega) in accordance with the manufacturer's instructions. Reactions were performed on three separate biological samples with each comprising technical triplicates. Primers were designed across the boundary of *Mfge8* exons 8 and 9, which are identical among the three mECap18 cell lines examined and were as follows: forward (GTATGTGGCGTCCTACAAGG) and reverse (GTGATGCGGTTATGCCAG). Cyclophilin was chosen as the internal standard, as it had primer efficiencies similar to the *Mfge8* gene of interest, and relative abundance was calculated using the $2^{-\Delta Ct}$ method [23].

Inhibition of extracellular vesicle cargo transfer to mouse spermatozoa

Three complementary strategies were assessed for their ability to inhibit protein transport from EVs to mouse spermatozoa. We first determined whether the EVs generated by *Mfge8* mutant mECap18 cell lines were refractory to sperm interaction. For this purpose, EVs were

isolated from each of three cell lines (one wild-type and two *Mfge8* mutant lines) before being labeled with biotinylation reagents and co-incubated with caput epididymal spermatozoa as described above. Secondly, we assessed the impact of competitive RGD-peptide mediated inhibition of EV-sperm interactions, whereby caput sperm were incubated with either 200 μM RGD tripeptide, 200 μM RAD control tripeptide (SCP0157 and SCP0156, respectively; Merck) or a PBS vehicle control. Incubations were conducted for 30 min at 37°C before the spermatozoa were washed and exposed to biotin labeled EVs. Co-incubation was continued for either 1 or 3 h at 37°C in 5% CO_2, after which spermatozoa were washed to remove unbound or peripherally adherent EVs and then fixed in 4% paraformaldehyde. Domains harboring transferred biotinylated proteins were detected using Alexa Fluor 488 conjugated streptavidin and confocal microscopy, and the percentage of labeled sperm recorded. The final strategy focused on the ability of antibody-mediated masking of the integrin alpha V receptor to perturb sperm-EV interactions. For this purpose, caput sperm were incubated in either anti-integrin alpha V antibodies (100 μg/mL), of the equivalent isotype-matched IgG (100 μg/mL) or a PBS vehicle control. After 40 min incubation at 37°C, spermatozoa were washed and exposed to biotin labeled EVs. Co-incubation was continued for either 1 or 3 h at 37°C in 5% CO_2, after which the sperm cells were washed, fixed and assessed for biotin transfer.

Statistical analyses

All experiments were replicated a minimum of three times, with pooled samples of spermatozoa and epididymosomes having been obtained from at least three male mice. For the purpose of assessing biotin labeling profiles, ≥ 100 spermatozoa were counted in each sample through blind assessment and the corresponding percentage of cells with post-acrosomal domain or whole head labeling was determined. Graphical data are presented as

mean values ± SEM. Statistical significance was determined using either a one-way ANOVA or two-way ANOVA with Tukey or Šidák correction for the appropriate multiple comparisons. Analysis was performed on GraphPad Prism version 8.4.3 for Windows (GraphPad Software, San Diego, CA).

RESULTS

The mECap18 cell line secretes an abundance of extracellular vesicles *in vitro*

Initial experiments focused on optimization of an immortalized mouse caput epididymal (mECap18) cell line as a model with which to study the mechanisms of EV-sperm interactions. Density gradient centrifugation of conditioned media harvested from cultured mECap18 cells yielded enriched populations of EVs (Fig. 1A; fractions 9 and 10) with a buoyant density equivalent to that of native epididymosomes [7]. These fractions tested positive for EV markers (FLOT1, CD9, CD63) by immunoblotting, and sizing analysis revealed they contained a relatively homogenous population (polydispersity indices of 0.24 and 0.25) of EVs of ~100 to 130 nm (Fig. 1B). Accordingly, fractions 9 and 10 were pooled and subjected to an additional suite of assays to confirm they contained EVs with characteristics that satisfied MISEV2018 guidelines [22]. Specifically, EVs were concentrated via adherence to aldehyde/sulfate latex beads enabling them to be visualized via labeling with anti-FLOT1 antibodies (Fig. 1C). Complementary ultrastructural analysis confirmed the spherical morphology, purity and size (~100 nm) of the EV preparations (Fig. 1D). Similarly, immunoblotting revealed the selective accumulation of EV markers (CD63 and CD9) relative to that of the parent mECap18 cells, the presence of additional EV markers (PSMD7, FLOT1 and GAPDH), and the absence of non-EV proteins (HSP90B1 and APOA1) (Fig. 1E) [22]. As an extension of this analysis, 2D SDS-PAGE demonstrated that the protein cargo encapsulated within mECap18 EVs is broadly similar to that of native mouse caput

epididymosomes (Fig. 2A-C); a result confirmed by immunoblotting detection of prominent epididymosome proteins (Fig. 2D) [14].

mECap18 extracellular vesicles selectively interact with mouse spermatozoa *in vitro*

In keeping with conserved physical and compositional properties among mECap18 EVs and epididymosomes, we next demonstrated these vesicles also share comparable functional characteristics. Specifically, differential labeling of mECap18 EVs with membrane impermeable and permeable biotinylation reagents confirmed that they are capable of transferring encapsulated protein cargo to recipient mouse spermatozoa. Thus, EVs pre-labeled with membrane impermeable biotin relayed protein to the post-acrosomal domain of ~40% of the sperm population (Fig. 3A,B). Equivalent patterns of protein transfer were detected in spermatozoa co-incubated with EVs pre-labeled with membrane permeable biotin, however, this was accompanied by additional foci of labeling extending into the anterior portion of the sperm head and distally into the flagellum (Fig. 3A,B). The specificity of protein transfer was attested by the complete absence of biotin staining in negative control populations of naïve sperm and in those cells incubated with non-biotinylated EVs (Fig. 3A). Conversely, direct biotinylation of spermatozoa yielded uniform labeling of all cells (Fig. 3A). We also confirmed that the macromolecular exchange mediated by mECap18 EVs extended beyond their protein cargo to encompass the miRNA sub-class of sncRNA. In this context, RT-qPCR revealed a significant increase in the abundance of several target miRNAs in spermatozoa post-incubation with mECap18 extracellular vesicles (Fig. 3C). Notably, an equivalent profile of miRNAs has previously been shown to be trafficked to sperm via epididymosomes [7], which together with conserved patterns of protein deposition, identify key functional parallels between mECap18 EVs and epididymosomes.

Targeted mutation of the *Mfge8* gene in mECap18 cells

The demonstration that mECap18 EVs replicate the functional properties of epididymosomes prompted the use of this model to explore the cognate receptor-ligand(s) that underpin sperm-EV interaction. Target selection for this study was, in part, guided by our previous work demonstrating that antibody masking of epididymosome-resident MFGE8 effectively reduces the ability of these vesicles to bind mouse spermatozoa [14]. CRISPR-Cas9 genome-editing was therefore used to generate mutant mECap18 cells harboring deletions in key sequences in the *Mfge8* gene that encode the functional domains of the MFGE8 protein. The ligand depleted EVs secreted by two such mutant cell lines were selected for further analysis.

Sequencing of these mutants demonstrated they harbored genomic deletions of either 7 base-pairs (bp) (mutant #1) or 283 bp (mutant #2) compared to the wild-type *Mfge8* gene (Fig. 4A). Both genomic deletions led to significant changes in the resultant transcripts, indicating that these deletions not only removed target sequence but also substantially altered the outcome of transcript splicing. Accordingly, PCR amplification and sequencing of the *Mfge8* cDNAs from mutant cell lines revealed that mutant #1 harbored to a complete deletion of exons 2 and 3 of the *Mfge8* gene (Fig. 4B,C and Supplementary Figure S1) and resulted in a single truncated protein product of approximately 30 kDa lacking both the EGF-like domains, and importantly, an integrin-binding RGD tripeptide motif (Fig. 4E,F,G). By contrast, mutant#2 was determined to result in deletions spanning exons 3 to 7, which yielded two alternatively spliced products (Fig. 4B,C and Supplementary Figure S1); the longer of which retained the RGD domain, while both products harbored truncated coagulation factor 5/8 domains (Fig. 4B,E). However, owing to the deletion of >90% of the target immunogen (Supplementary Figure S1), the anti-MFGE8 antibodies used in this study failed to detect either of the truncated protein products produced by the mutant #2 mECap18 cell line via immunoblotting (Fig 4F,G). Nevertheless, RT-qPCR confirmed that levels of *Mfge8* gene

expression levels were indistinguishable among wild-type and the two mutant mECap18 cell lines (Fig. 4D).

Loss of the MFGE8 RGD binding motif compromises sperm-extracellular vesicle interaction

To examine whether the introduced *Mfge8* mutations had any bearing on the efficacy of sperm-EV interaction, ligand depleted EVs pre-labeled with membrane impermeable biotin were co-incubated with caput spermatozoa. Notably, the mutations harbored by both mutant #1 and mutant #2 cell lines significantly ($P \leq 0.05$) compromised the efficacy of sperm-EV interaction (Fig. 5A). This result was most pronounced in EVs totally lacking an MFGE8 RGD domain (mutant #1), which transferred biotin label to ~60% fewer spermatozoa than that of EVs recovered from wild-type mECap18 cells. Moreover, biotinylated protein transfer from mutant #1 EVs was restricted to the sub-acrosomic ring (Fig. 5B), distinct from the post-acrosomal labeling witnessed in EVs generated by either wild-type or mutant #2 mECap18 cells. Although not as pronounced, the transfer of mutant #1 EV proteins labeled with membrane permeable biotin (i.e. comprising both encapsulated proteins and those expressed on the vesicle membrane) was also significantly reduced compared to that of wild-type EV proteins at both 1 and 3 h post-incubation (Fig 5C). Furthermore, when considering the fate of these EV proteins, it was revealed that those originating from mutant #1 EVs showed minimal redistribution beyond their deposition into the post-acrosomal domain of the sperm head during the 3 h co-incubation period (Fig. 5D). By contrast, those proteins trafficked to spermatozoa via wild-type or mutant #2 EVs were shown to undergo a pronounced redistribution throughout the sperm head between 1 and 3 h post-incubation [as has previously been shown for epididymosome proteins [10]].

Based on these collective data we infer that, mutant #1 EVs display a reduced ability to engage the downstream signaling/fusion machinery needed to permit efficient uptake of their encapsulated cargo. Moreover, the absence of an equivalent response in mutant #2 EVs, implicates the RGD motif as being a key mediator of this phenomenon. Accordingly, pre-absorption of sperm receptors with the RGD tripeptide proved effective in significantly attenuating the subsequent uptake (Fig. 5F), and the redistribution (Fig. 5G), of biotinylated proteins following co-incubation with wild-type EVs. By comparison, pre-incubation of spermatozoa with an equivalent amount of RAD control tripeptide had no effect on the transfer or redistribution of EV proteins (Fig. 5F,G).

αV integrins participate in sperm-extracellular vesicle interaction

Whilst αV integrins have been implicated as putative receptors for both the MFGE8 RGD motif [24], and the tethering of oviductal derived EVs to spermatozoa [25], it is not known if these receptors also mediate the equivalent adhesion of epididymal EVs to spermatozoa. Here, we demonstrate the presence and distribution of αV integrin in mouse spermatozoa, revealing that the protein localizes to the peri-acrosomal domain and mid-piece of the tail in fixed permeabilized cells (Fig. 5J). Despite this localization profile differing from that of the initial site of EV adhesion, pre-labeling of mouse spermatozoa with an αV function blocking antibody (RMV-7) [26], resulted in a significant reduction in biotinylated protein transfer from wild-type EVs after 1 h (Fig. 5H). This strategy also reduced the redistribution of biotinylated EV protein after 3 h of co-incubation (Fig. 5I) compared with mock assays (i.e. sperm pre-incubated with PBS). The specificity of this response was attested by the absence of an effect in sperm pre-labeled with non-immune IgG (Fig. 5H,I).

DISCUSSION

There is mounting evidence that epididymosomes play a fundamental role in modulating sperm function via the exchange of fertility modulating proteins and epigenetic cargo [3]. Nevertheless, the mechanisms that facilitate the selective adhesion and subsequent uptake of the epididymosome payload into recipient spermatozoa have yet to be fully resolved. There is however, general consensus that, as with other forms of EVs, the initial binding of epididymosomes is mediated by cellular protein receptors, and their cognate ligand(s) on the vesicle membrane; with our previous work having implicated MFGE8 as one such ligand [14]. Accordingly, ultrastructural analyses demonstrated that MFGE8 localization extends from the epididymosome surface into stalk-like projections associated with sites of epididymosome-sperm interaction [14]. Furthermore, antibody masking of MFGE8 ligands compromises the efficiency of epididymosome-mediated protein transfer to recipient spermatozoa [14]. Here, we provide critical new evidence implicating MFGE8 in the efficient exchange of macromolecular EV cargo to mouse spermatozoa, with our data identifying the RGD motif as being of particular importance in mediating this interaction.

MFGE8 is synthesized as a ~53 kDa glycoprotein possessing a cleavable signal peptide, followed immediately by two N-terminal epidermal growth factor (EGF)-like repeats and two C-terminal discoidin/F5/8C domains. The second EGF domain also contains the RGD integrin-binding motif, which is known to engage αvβ3/5 integrin heterodimers to facilitate cell adhesion and induce integrin-mediated signal transduction [17]. In the mouse, MFGE8 is also produced as a ~66 kDa splice variant that includes an additional 37 amino acid proline/threonine-rich sequence, which may increase the binding efficiency to phospholipids and/or increase the efficiency of secretion. Expression of the two splice variants shows spatial and temporal specificity, with both isoforms being produced in the epididymis and represented in epididymosomes and, to a lesser extent in mECap EVs in

which the lower molecular weight isoform predominates. This is in contrast to the exclusive secretion of the long isoform that has previously been described for epidermal keratinocytes [27].

In terms of its function within the male reproductive tract, MFGE8 was originally characterized as a sperm protein with binding affinity for zona pellucida glycoproteins [18]. However, MFGE8 has also been implicated in the support of epididymal cell adhesion via RGD binding to αV integrin receptors on epididymal epithelial cells; a finding that accounts for the pronounced epididymal epithelium pathologies that accompany the loss of MFGE8 function [24, 28]. In spermatozoa, we hypothesize that the RGD-αV integrin interaction may stimulate intracellular signaling pathways that underpin the recruitment of lipid rafts, and their associated fusion machinery, to sites of EV docking. Indeed, we have previously shown that co-incubation of caput spermatozoa with epididymosomes can promote sequestration of lipid raft markers within the post-acrosomal domain [10]. In addition to offering insight into the receptors that putatively drive this translocation, our studies also raise the intriguing prospect that deficits in ZP adhesion documented in *Mfge8* null males [19] may, at least in part, be attributed to inefficient transfer / uptake of epididymosome cargo as opposed to resting entirely with a defect in MFGE8. Notably, the presence of MFGE8 orthologues, each possessing conserved RGD domains, in other species (such as the human, rat, bovine and porcine; Supplementary Figure S2) raises the prospect that this protein may fulfil equivalent functional roles across the mammalian lineage.

Nevertheless, whilst our data implicates MFGE8 in EV interaction, they also suggest that this protein is unlikely to be the sole ligand responsible for regulating EV adhesion. Thus, our collective interventional data point to a suppression, as opposed to elimination, of EV interaction by blocking of MFGE8 function. These data accord with independent evidence that MFGE8 represents a virtually ubiquitously membrane component of exosomes

secreted from all cell types thus far examined [29]; including mammary fat globules released into milk, as well as the epididymosomes secreted from non-rodent species [30]. It is therefore considered likely that alternative ligands are important in guiding the specificity, and perhaps efficiency, of sperm-epididymosome interactions. In this sense, it has been shown that exosomes isolated from MFGE8-deficient mice are nearly as efficient in transferring antigen/MHC complexes to recipient dendritic cells as vesicles isolated from wild-type mice [31]. Thus, despite the adhesive properties of MFGE8, the protein has been proposed to fulfil ancillary roles in terms of the formation and/or secretion of EVs. Consistent with this model, transfection of COS-7 cells with the full-length *Mfge8* coding sequence increases exosome secretion by a factor of 3- to 4-fold [32]. Conversely, expression of mutant constructs with either the C-terminal F5/8C domain deleted, abolished both the cell-surface and exosome localizations of the MFGE8 protein, whilst the C2 domain has been demonstrated essential for increased exosome secretion [32].

Notwithstanding these data, our collective evidence suggests that MFGE8 association with exosomes has additional functional significance in terms of supporting EV adhesion and/or uptake at the surface of recipient cells. Indeed, the broad conservation of MFGE8 among exosomes of varied cellular origin may account for why spermatozoa are able to interact in an efficient manner with exosomes isolated from non-reproductive cell lines such as those derived from the human embryonic kidney (i.e. HEK293T cells) [33]. In this sense, HEK293T exosomes have been shown to be internalized into boar spermatozoa within as little as 10 min of co-incubation; with no significant deleterious effects on basic sperm function [33]. Such findings raise the intriguing prospect of being able to harness EVs, laden with cell adhesion molecules such as MFGE8, as versatile research tools for studying sperm biology and as a prescient for developing vectors capable of delivering therapeutic payloads for the treatment of male infertility.

DATA AVAILABILITY STATEMENT

The data that supports the findings of this study are available in the supplementary material of this article.

DECLARATIONS OF INTEREST

The authors have no competing interests to declare

AUTHOR CONTRIBUTIONS

NAT, SJS, WZ, DAS-B, PS performed the experimental work and data analysis. NAT, MDD, ALE, GND, EGB, SDR, and BN each contributed to the conceptualization, literature curation, and drafting of the manuscript. All authors edited the manuscript and approved the final version of the manuscript.

FUNDING

This research was supported by the award of a National Health and Medical Research Council of Australia (NHMRC) Project Grant awarded to BN and MDD (APP1147932). BN, MDD and EGB are recipients of NHMRC Research Fellowships.

Figure Legends

Figure 1. Characterization of mECap18 extracellular vesicles. mECap18 cell supernatant was fractionated by density gradient ultracentrifugation followed by the recovery and characterization of 12 equal fractions. **A)** Immunoblot analysis was performed to detect the distribution of fractions containing the characteristic EV markers of FLOT1, CD63 and CD9. **B)** On the basis of the analysis, EVs partitioning into fractions 9 - 10 were individually assessed for size heterogeneity via dynamic light scattering measurement of mean particle size. Data are reported as mean particle size (columns) and polydispersity index values (numbers above columns), whereby the lower the value the more homogenous the preparation. EVs were subsequently pooled from fractions 9 and 10, and either **C)** immobilized onto a solid support matrix consisting of aldehyde/sulphate latex beads before being sequentially labeled with anti-FLOT1 and appropriate Alexa Fluor 488 conjugated secondary antibodies (green; scale bar = 20 μm), **D)** visualized by transmission electron microscopy (scale bar = 200 nm), or **E)** prepared for immunoblotting alongside complete mECap18 cell lysates (Cell) with the EV specific markers of CD63, CD9, PSMD7, FLOT1, negative controls of HSP90B1 and APOA1 and the loading control of GAPDH. All experiments were replicated three times on independent samples and depicted are representative images and immunoblots.

Trigg et al., Figure 1

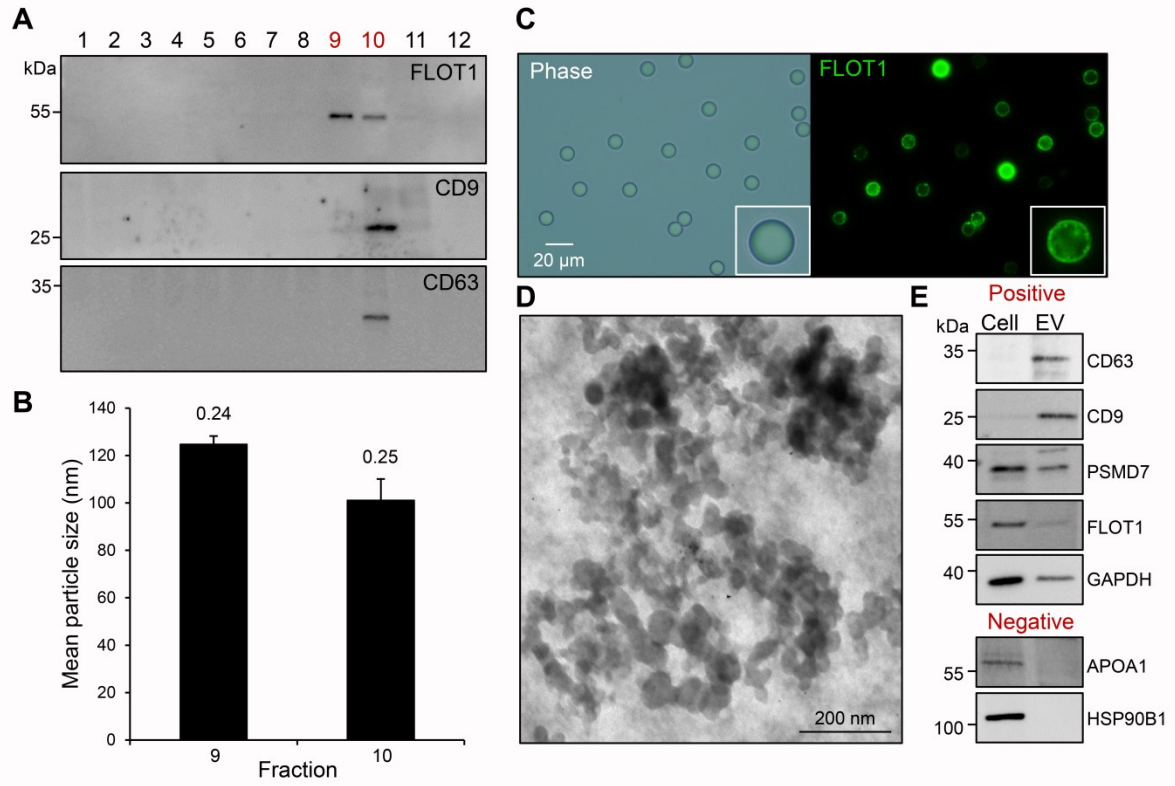

Figure 2. Conservation of mECap18 extracellular vesicles and mouse epididymosome proteomes. A-C) The proteomic profile of mECap18 EVs (Cy5, red) and mouse caput epididymosomes (Cy3, green) was assessed via labeling of protein extracts with size and charge matched cyanine-dyes. Labeled proteins were mixed in equal proportion, resolved by 2D SDS-PAGE and visualized. **D)** Immunoblots of mECap18 EVs and mouse caput epididymosomes were probed with antibodies against abundant epididymosome proteins. All experiments were replicated three times on independent samples and depicted are representative gel images and immunoblots.

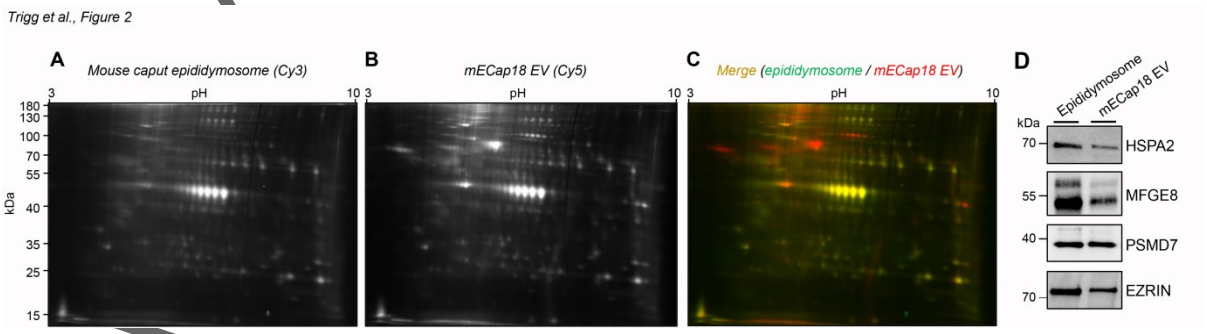

Figure 3. mECap18 extracellular vesicle interaction with mouse spermatozoa. A) The exchange of proteins from mECap18 EVs to mouse spermatozoa was assessed via pre-labeling EVs with either membrane permeable or impermeable biotinylation reagents. After co-incubation, spermatozoa were assessed for protein uptake via affinity labeling with Alexa Fluor 488 conjugated streptavidin. Controls included spermatozoa incubated without EVs, with these cells either being left in an unlabeled state to serve as negative controls or directly labeled with biotin to confirm the specificity of EV-mediated protein transfer. **B)** Protein transfer was quantified by assessing the number of spermatozoa displaying fluorescent labeling. **C)** Transfer of alternate EV cargo, in the form of miRNAs, was also assessed via the extraction of total sperm RNA pre- and post-incubation followed by RT-qPCR amplification of target miRNAs. All graphical data are presented as means ± SEM. Expression levels of target miRNAs were normalized against the U6 small nuclear RNA control. * $P \leq 0.05$, ** $P \leq 0.01$

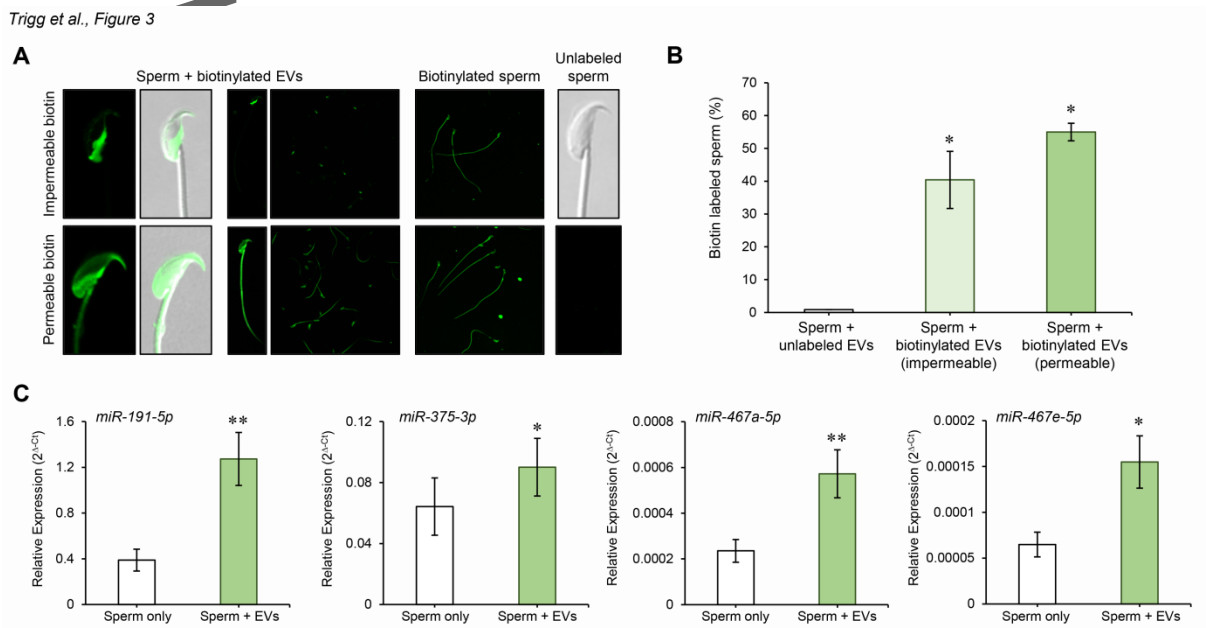

Figure 4. Characterization of CRISPR/Cas9 mediated *Mfge8* mutations. mECap18 cells were transfected with a 20 bp Trueguide gRNA targeting the center of exon 3 of *Mfge8*, upstream of the RGD motif. Individual clones were isolated and grown using a limited dilution strategy and subsequently sequenced to determine genotype. **A)** Resultant genomic DNA sequencing flanking the gRNA target (red box) enabled identification of two mutant lines with 7 bp and 283 bp genomic deletions (mutant #1 and mutant #2), respectively compared to wild-type. **B)** Intron/Exon mapping generated from Sanger sequencing of subcloned cDNA amplicons revealed complete deletion of exons 2 and 3 from mutant #1 (Δ exons 2-3) and a deletion spanning exons 3 to 7 from the alternately spliced mutant #2 (Δ exons 3-7) mutant cell lines. **C)** Resolution of the mutant cDNA by agarose gel electrophoresis revealed amplicons of the expected size. **D)** Moreover, RT-qPCR analysis confirmed equivalent expression of wild-type and mutant *Mfge8* transcripts. Graphical data are presented are as transformed values (mean ± SEM) calculated via the $2e^{-\Delta C(t)}$ method and are representative of three biological replicates (with each comprising three technical replicates). **E)** Schematic of the predicted domain structure for MFGE8 protein products derived from CRISPR/Cas9 gene editing, illustrating the predicted loss of a 159 amino acids from the protein product of mutant #1 (Δ 159 AA) and of either of 234 or 262 amino acids from mutant #2 (Δ 234 AA and Δ 262 AA). **F)** Extracellular vesicles were harvested from wild-type and mutant mECap18 cell lines prior to being lysed in (3-[(3-cholamidopropyl] dimethylammonio)-1-propanesulfonate (CHAPS) detergent and solubilized protein prepared for immunoblotting with anti-MFGE8 antibodies. This analysis revealed the presence of a single truncated protein product of approximately 30 kDa generated from the mutant #1 mECap18 cell line. By contrast, the deletion of >90% of the target immunogen (Supplementary Figure S1), prevented the detection of the truncated protein products produced by the mutant #2 mECap18 cell line. **G)** These was result was confirmed by

immunoblotting of extracellular vesicles proteins prepared with a more stringent SDS-based solubilization protocol.

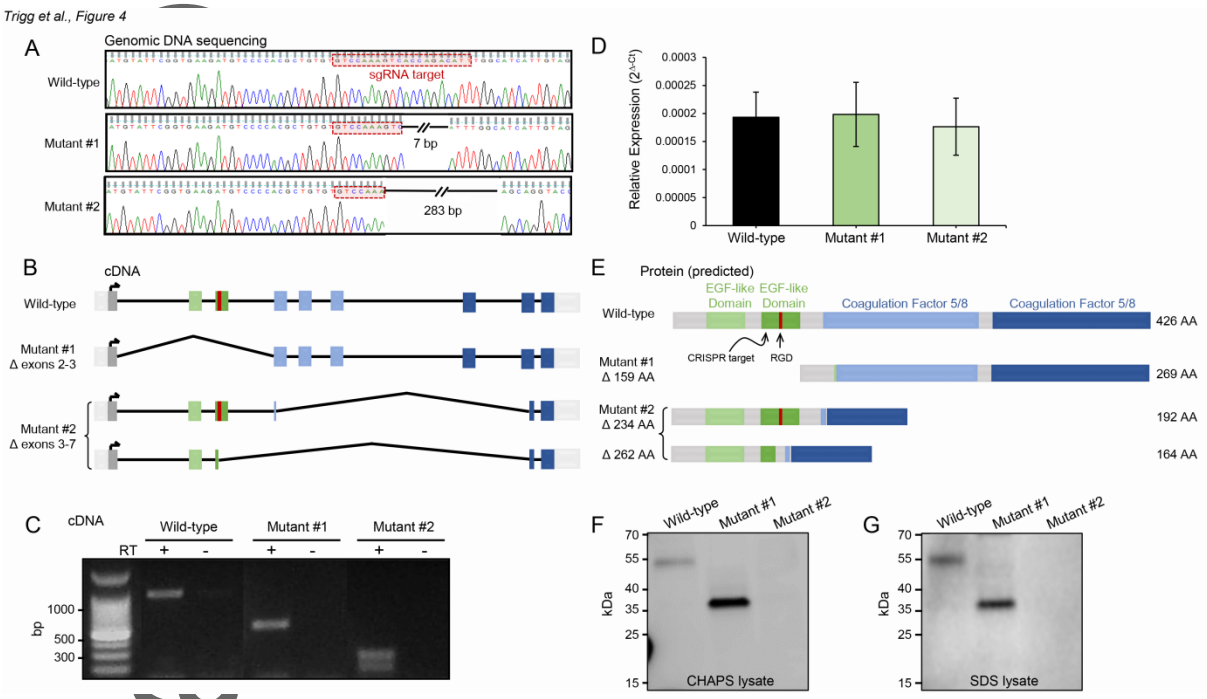

Figure 5. Characterization of the role of MFGE8 – integrin αV in sperm extracellular vesicle interactions. EVs generated from wild-type and mutant *Mfge8* mECap18 cells, were pre-labeled with either **(A-B)** membrane impermeable or **(C-E)** membrane permeable biotin prior to co-incubation with caput epididymal spermatozoa to assess the efficacy of sperm-EV interaction. **A-E)** Spermatozoa harboring biotin label were quantified, and the relative distribution of label assessed post-incubation times of 1 and 3 h. **F-G)** To examine the role of the RGD motif in sperm-EV interaction, caput epididymal spermatozoa were pre-treated with either an RGD or RAD control tripeptide before introduction of EVs harvested from wild-type mECap18 cells. The sperm were then assessed for biotin uptake and distribution. **H-I)** Alternatively, the role of αV integrin in sperm-EV adhesion was evaluated using a similar strategy in which sperm were pre-labeled with either an αV function blocking antibody or non-immune IgG. **J)** Immunofluorescence was utilized to examine the presence and distribution of αV integrin in mouse spermatozoa. All graphical data are presented as means ± SEM, statistical significance was determined using either a **A)** one-way ANOVA or **C-D, F-I)** a two-way ANOVA with Tukey or Šidák correction for the appropriate multiple comparisons. **A, C, F, H)** Statistical differences of $P \leq 0.05$ are denoted by differing letters. **D, G, I)** * $P \leq 0.05$ ** $P \leq 0.01$ *** $P \leq 0.001$.

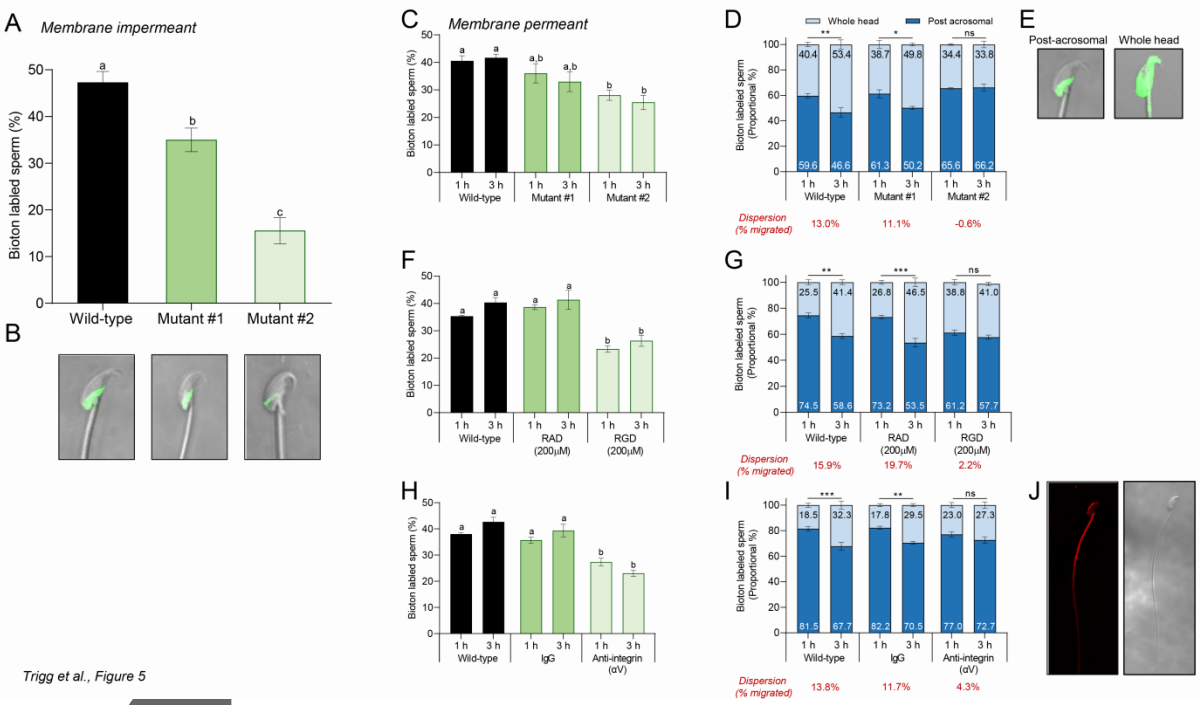

Trigg et al., Figure 5

REFERENCES

[1] A. T. Reid, K. Redgrove, R. J. Aitken,B. Nixon, Asian J Androl 2011, 13, 88.

[2] L. Hermo, R. M. Pelletier, D. G. Cyr,C. E. Smith, Microsc Res Tech 2010, 73, 241.

[3] B. Nixon, S. L. Cafe, A. L. Eamens, G. N. De Iuliis, E. G. Bromfield, J. H. Martin, D. A. Skerrett-Byrne,M. D. Dun, Mol Cell Endocrinol 2020, *In press*.

[4] R. J. Aitken, B. Nixon, M. Lin, A. J. Koppers, Y. H. Lee,M. A. Baker, Asian J Androl 2007, 9, 554.

[5] B. Nixon, G. N. De Iuliis, M. D. Dun, W. Zhou, N. A. Trigg,A. L. Eamens, Andrology 2019, 7, 669.

[6] W. Zhou, G. N. De Iuliis, M. D. Dun,B. Nixon, Front Endocrinol (Lausanne) 2018, 9, 59.

[7] J. N. Reilly, E. A. McLaughlin, S. J. Stanger, A. L. Anderson, K. Hutcheon, K. Church, B. P. Mihalas, S. Tyagi, J. E. Holt, A. L. Eamens,B. Nixon, Sci Rep 2016, 6, 31794.

[8] H. Rejraji, B. Sion, G. Prensier, M. Carreras, C. Motta, J. M. Frenoux, E. Vericel, G. Grizard, P. Vernet,J. R. Drevet, Biol Reprod 2006, 74, 1104.

[9] R. Sullivan, Asian J Androl 2015, 17, 726.

[10] W. Zhou, S. J. Stanger, A. L. Anderson, I. R. Bernstein, G. N. De Iuliis, A. McCluskey, E. A. McLaughlin, M. D. Dun,B. Nixon, BMC Biol 2019, 17, 35.

[11] C. Belleannee, E. Calvo, J. Caballero,R. Sullivan, Biol Reprod 2013, 89, 30.

[12] R. Sullivan, G. Frenette,J. Girouard, Asian J Androl 2007, 9, 483.

[13] G. Frenette, J. Girouard,R. Sullivan, Biol Reprod 2006, 75, 885.

[14] B. Nixon, G. N. De Iuliis, H. M. Hart, W. Zhou, A. Mathe, I. Bernstein, A. L. Anderson, S. J. Stanger, D. A. Skerrett-Byrne, M. F. B. Jamaluddin, J. G. Almazi, E. G. Bromfield, M. R. Larsen,M. D. Dun, Mol Cell Proteomics 2019, 18, S91

[15] K. Hutcheon, E. A. McLaughlin, S. J. Stanger, I. R. Bernstein, M. D. Dun, A. L. Eamens,B. Nixon, RNA Biol 2017, 14, 1776.

[16] J. Girouard, G. Frenette,R. Sullivan, Int J Androl 2011, 34, e475.

[17] A. Raymond, M. A. Ensslin,B. D. Shur, J Cell Biochem 2009, 106, 957.

[18] M. Ensslin, T. Vogel, J. J. Calvete, H. H. Thole, J. Schmidtke, T. Matsuda,E. Topfer-Petersen, Biol Reprod 1998, 58, 1057.

[19] M. A. Ensslin,B. D. Shur, Cell 2003, 114, 405.

[20] P. Sipila, R. Shariatmadari, I. T. Huhtaniemi,M. Poutanen, Endocrinology 2004, 145, 437; W. Zhou, G. N. De Iuliis, A. P. Turner, A. T. Reid, A. L. Anderson, A. McCluskey, E. A. McLaughlin,B. Nixon, Biol Reprod 2017, 96, 159.

[21] A. T. Reid, A. L. Anderson, S. D. Roman, E. A. McLaughlin, A. McCluskey, P. J. Robinson, R. J. Aitken,B. Nixon, FASEB J 2015, 29, 2872.

[22] C. Thery, K. W. Witwer, E. Aikawa, M. J. Alcaraz, J. D. Anderson, R. Andriantsitohaina, A. Antoniou, T. Arab, F. Archer, G. K. Atkin-Smith, D. C. Ayre, J. M. Bach, D. Bachurski, H. Baharvand, L. Balaj, S. Baldacchino, N. N. Bauer, A. A. Baxter, M. Bebawy, C. Beckham, A. Bedina Zavec, A. Benmoussa, A. C. Berardi, P. Bergese, E. Bielska, C. Blenkiron, S. Bobis-Wozowicz, E. Boilard, W. Boireau, A. Bongiovanni, F. E. Borras, S. Bosch, C. M. Boulanger, X. Breakefield, A. M. Breglio, M. A. Brennan, D. R. Brigstock, A. Brisson, M. L. Broekman, J. F. Bromberg, P. Bryl-Gorecka, S. Buch, A. H. Buck, D. Burger, S. Busatto, D. Buschmann, B. Bussolati, E. I. Buzas, J. B. Byrd, G. Camussi, D. R. Carter, S. Caruso, L. W. Chamley, Y. T. Chang, C. Chen, S. Chen, L. Cheng, A. R. Chin, A. Clayton, S. P. Clerici, A. Cocks, E. Cocucci, R. J. Coffey, A. Cordeiro-da-Silva, Y. Couch, F. A. Coumans, B. Coyle, R. Crescitelli, M. F. Criado, C. D'Souza-Schorey, S. Das, A. Datta Chaudhuri, P. de Candia, E. F. De Santana, O. De Wever, H. A. Del Portillo, T.

Demaret, S. Deville, A. Devitt, B. Dhondt, D. Di Vizio, L. C. Dieterich, V. Dolo, A. P. Dominguez Rubio, M. Dominici, M. R. Dourado, T. A. Driedonks, F. V. Duarte, H. M. Duncan, R. M. Eichenberger, K. Ekstrom, S. El Andaloussi, C. Elie-Caille, U. Erdbrugger, J. M. Falcon-Perez, F. Fatima, J. E. Fish, M. Flores-Bellver, A. Forsonits, A. Frelet-Barrand, F. Fricke, G. Fuhrmann, S. Gabrielsson, A. Gamez-Valero, C. Gardiner, K. Gartner, R. Gaudin, Y. S. Gho, B. Giebel, C. Gilbert, M. Gimona, I. Giusti, D. C. Goberdhan, A. Gorgens, S. M. Gorski, D. W. Greening, J. C. Gross, A. Gualerzi, G. N. Gupta, D. Gustafson, A. Handberg, R. A. Haraszti, P. Harrison, H. Hegyesi, A. Hendrix, A. F. Hill, F. H. Hochberg, K. F. Hoffmann, B. Holder, H. Holthofer, B. Hosseinkhani, G. Hu, Y. Huang, V. Huber, S. Hunt, A. G. Ibrahim, T. Ikezu, J. M. Inal, M. Isin, A. Ivanova, H. K. Jackson, S. Jacobsen, S. M. Jay, M. Jayachandran, G. Jenster, L. Jiang, S. M. Johnson, J. C. Jones, A. Jong, T. Jovanovic-Talisman, S. Jung, R. Kalluri, S. I. Kano, S. Kaur, Y. Kawamura, E. T. Keller, D. Khamari, E. Khomyakova, A. Khvorova, P. Kierulf, K. P. Kim, T. Kislinger, M. Klingeborn, D. J. Klinke, 2nd, M. Kornek, M. M. Kosanovic, A. F. Kovacs, E. M. Kramer-Albers, S. Krasemann, M. Krause, I. V. Kurochkin, G. D. Kusuma, S. Kuypers, S. Laitinen, S. M. Langevin, L. R. Languino, J. Lannigan, C. Lasser, L. C. Laurent, G. Lavieu, E. Lazaro-Ibanez, S. Le Lay, M. S. Lee, Y. X. F. Lee, D. S. Lemos, M. Lenassi, A. Leszczynska, I. T. Li, K. Liao, S. F. Libregts, E. Ligeti, R. Lim, S. K. Lim, A. Line, K. Linnemannstons, A. Llorente, C. A. Lombard, M. J. Lorenowicz, A. M. Lorincz, J. Lotvall, J. Lovett, M. C. Lowry, X. Loyer, Q. Lu, B. Lukomska, T. R. Lunavat, S. L. Maas, H. Malhi, A. Marcilla, J. Mariani, J. Mariscal, E. S. Martens-Uzunova, L. Martin-Jaular, M. C. Martinez, V. R. Martins, M. Mathieu, S. Mathivanan, M. Maugeri, L. K. McGinnis, M. J. McVey, D. G. Meckes, Jr., K. L. Meehan, I. Mertens, V. R. Minciacchi, A. Moller, M. Moller Jorgensen, A. Morales-

Kastresana, J. Morhayim, F. Mullier, M. Muraca, L. Musante, V. Mussack, D. C. Muth, K. H. Myburgh, T. Najrana, M. Nawaz, I. Nazarenko, P. Nejsum, C. Neri, T. Neri, R. Nieuwland, L. Nimrichter, J. P. Nolan, E. N. Nolte-'t Hoen, N. Noren Hooten, L. O'Driscoll, T. O'Grady, A. O'Loghlen, T. Ochiya, M. Olivier, A. Ortiz, L. A. Ortiz, X. Osteikoetxea, O. Ostergaard, M. Ostrowski, J. Park, D. M. Pegtel, H. Peinado, F. Perut, M. W. Pfaffl, D. G. Phinney, B. C. Pieters, R. C. Pink, D. S. Pisetsky, E. Pogge von Strandmann, I. Polakovicova, I. K. Poon, B. H. Powell, I. Prada, L. Pulliam, P. Quesenberry, A. Radeghieri, R. L. Raffai, S. Raimondo, J. Rak, M. I. Ramirez, G. Raposo, M. S. Rayyan, N. Regev-Rudzki, F. L. Ricklefs, P. D. Robbins, D. D. Roberts, S. C. Rodrigues, E. Rohde, S. Rome, K. M. Rouschop, A. Rughetti, A. E. Russell, P. Saa, S. Sahoo, E. Salas-Huenuleo, C. Sanchez, J. A. Saugstad, M. J. Saul, R. M. Schiffelers, R. Schneider, T. H. Schoyen, A. Scott, E. Shahaj, S. Sharma, O. Shatnyeva, F. Shekari, G. V. Shelke, A. K. Shetty, K. Shiba, P. R. Siljander, A. M. Silva, A. Skowronek, O. L. Snyder, 2nd, R. P. Soares, B. W. Sodar, C. Soekmadji, J. Sotillo, P. D. Stahl, W. Stoorvogel, S. L. Stott, E. F. Strasser, S. Swift, H. Tahara, M. Tewari, K. Timms, S. Tiwari, R. Tixeira, M. Tkach, W. S. Toh, R. Tomasini, A. C. Torrecilhas, J. P. Tosar, V. Toxavidis, L. Urbanelli, P. Vader, B. W. van Balkom, S. G. van der Grein, J. Van Deun, M. J. van Herwijnen, K. Van Keuren-Jensen, G. van Niel, M. E. van Royen, A. J. van Wijnen, M. H. Vasconcelos, I. J. Vechetti, Jr., T. D. Veit, L. J. Vella, E. Velot, F. J. Verweij, B. Vestad, J. L. Vinas, T. Visnovitz, K. V. Vukman, J. Wahlgren, D. C. Watson, M. H. Wauben, A. Weaver, J. P. Webber, V. Weber, A. M. Wehman, D. J. Weiss, J. A. Welsh, S. Wendt, A. M. Wheelock, Z. Wiener, L. Witte, J. Wolfram, A. Xagorari, P. Xander, J. Xu, X. Yan, M. Yanez-Mo, H. Yin, Y. Yuana, V. Zappulli, J. Zarubova, V. Zekas, J. Y.

Zhang, Z. Zhao, L. Zheng, A. R. Zheutlin, A. M. Zickler, P. Zimmermann, A. M. Zivkovic, D. Zocco,E. K. Zuba-Surma, J Extracell Vesicles 2018, 7, 1535750.

[23] T. D. Schmittgen,K. J. Livak, Nat Protoc 2008, 3, 1101.

[24] A. S. Raymond, B. Elder, M. Ensslin,B. D. Shur, Mol Reprod Dev 2010, 77, 550.

[25] A. A. Al-Dossary, P. Bathala, J. L. Caplan,P. A. Martin-DeLeon, J Biol Chem 2015, 290, 17710.

[26] K. Takahashi, T. Nakamura, M. Koyanagi, K. Kato, Y. Hashimoto, H. Yagita,K. Okumura, J Immunol 1990, 145, 4371.

[27] T. Watanabe, R. Totsuka, S. Miyatani, S. Kurata, S. Sato, I. Katoh, S. Kobayashi,Y. Ikawa, Cell Tissue Res 2005, 321, 185.

[28] A. S. Raymond,B. D. Shur, J Cell Sci 2009, 122, 849.

[29] K. Denzer, M. J. Kleijmeer, H. F. Heijnen, W. Stoorvogel,H. J. Geuze, J Cell Sci 2000, 113 Pt 19, 3365.

[30] J. L. Gatti, S. Metayer, M. Belghazi, F. Dacheux,J. L. Dacheux, Biol Reprod 2005, 72, 1452.

[31] P. Veron, E. Segura, G. Sugano, S. Amigorena,C. Thery, Blood Cells Mol Dis 2005, 35, 81.

[32] K. Oshima, N. Aoki, T. Kato, K. Kitajima,T. Matsuda, Eur J Biochem 2002, 269, 1209.

[33] T. Vilanova-Perez, C. Jones, S. Balint, R. Dragovic, L. D. M, M. Yeste,K. Coward, Nanomedicine (Lond) 2020.